AUTOMATED CFD TOOLS FOR THE DESIGN OF MARINE PROPULSION SYSTEMS

Vladimir Krasilnikov[1], Benedetto Di Paolo[2] and Lisandro Maders[3]
[1] SINTEF Ocean AS, Trondheim, Norway,
[2] ENGYS Srl, Trieste, Italy
[3] ENGYS Ltda., Porto Alegre, Brazil
vladimir.krasilnikov@sintef.no, b.dipaolo@engys.com, l.maders@engys.com

INTRODUCTION

Modern ship propulsion requires accurate prediction of propulsor performance not only at the design point but also in off-design conditions (e.g., heavy loading with cavitation onset, large pod heading angles, and off-design pitch of controlled-pitch (*CP*) propellers). Because viscosity governs the flow physics in such scenarios, potential-flow tools are insufficient; viscous CFD must be integrated in the design loop. This work summarizes a workflow that embeds HELYX® into SINTEF Ocean's AKPA suite to automate geometry handling, meshing, solution setup, and post-processing for open, ducted and podded propulsors, including non-cavitating and cavitating regimes validated against SINTEF Ocean model tests.

MATERIALS AND METHODS

In AKPA, preliminary blade/hub design is performed with lifting-surface and panel methods; CFD is then used to assess off-design behavior, refine blade/hub details (edges, tip, root, hub cap), and verify risks related to cavitation, pressure pulses and noise.

In terms of geometry preparation, AKPA exports blades, hubs, ducts, rudders and pod gear-housings as STL/STEP using B-spline surfaces; HELYX reads these parts, extracts feature curves for local refinement, can include third-party components, and auto-generates the computational domain, volumetric refinements and (for sliding-mesh cases) rotating regions.

The automated setup uses *helyxHexMesh* with the *Extrude* algorithm to create hex-dominant meshes with robust prism-layer growth. Compared with *snappyHexMesh*-like workflow in OpenFOAM, *Extrude* builds a thin boundary layer before snapping, adds all prism layers in one pass, and optimizes sphericity, enabling 100% layer coverage even at thin edges, tips, blade/duct clearance and hub gaps (Figs. 3–4). Typical guidance: model scale wall-resolved $y+ \approx 1$ with 8–10 layers; full-scale wall-modelled $y+ \approx 50-70$ with ~10–12 layers. Refinement levels are set on features/surfaces/volumes relative to a base size tied to diameter D; global mesh factors enable systematic sensitivity studies.

Turbulence closure was modelled using the RANS $k-\omega$ SST model. Motion is handled by *MRF* (Moving Reference Frame) for single open propellers (and moderately loaded ducted propellers in uniform flow) and by Sliding Mesh (*SM*) with *AMI* (Arbitrary Mesh Interface) for pods, propeller-rudder systems, counter-rotating units, and generally for ducted propellers when recirculation/separation make the flow unsteady. Non-cavitating cases use the unified solver helyxSolve (*SIMPLE* for steady *MRF*, *PIMPLE* for unsteady *SM*). Cavitation is simulated with *interPhaseChangeFoamDyMFoam* (which will be integrated within HELYX *helyxSolve* solver framework in future) in a two-stage procedure: a forced non-cavitating spin-up (≈5 rev, 2°/step), ramp of saturation pressure (≈0.5 rev), then cavitating stage (5–10 rev, ≥1°/step) with the *Schnerr–Sauer* model (default seed settings).

RESULTS

Two test cases were analyzed: the open propeller P1380 in open water conditions, with and without cavitation; and the ducted azimuth thruster P1374 with *CP* propeller. The four-blade high-skew *CP* propeller P1380 (design $P(0.7)/D$=1.188) was model-tested in SINTEF's cavitation tunnel. The paper compares CFD and EFD open-water characteristics (Fig. 1) from tests with different diameters, rig configurations (push/pull), and Reynolds numbers. The CFD used a steady MRF model of a single blade passage at 20 Hz (push rig), default mesh factor, ≈2.95 M cells; thrust and torque coefficients agreed with experiments within ~6%, while open-water efficiency was under-predicted attributed to transition present in EFD but not in fully-turbulent CFD. Cavitation effects on loads at

J=0.6 and J=0.2 (Figure 2) were obtained with the two-stage cavitation procedure; a mesh-refinement study indicated practical convergence at the default mesh, and realistic trends even on the coarsest grid. Qualitative agreement of cavity extents vs. $\sigma_{\eta D}$ is shown in Figure 3 (only for $\sigma_{\eta D}$ = 1.5, 3.0 and 4.0 due to size limitations).

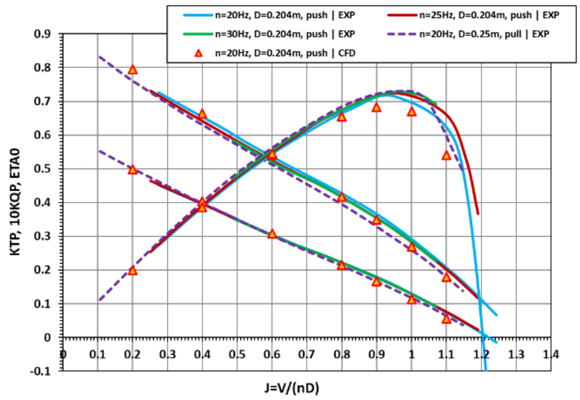

Fig. 1. Open water characteristic of the propeller P1380. P/D=1.188. Atmospheric conditions.

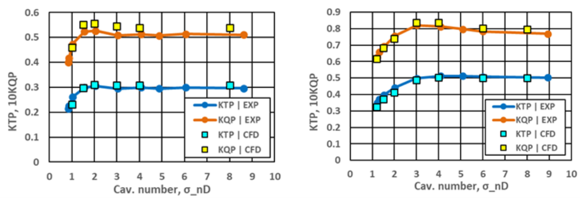

Figure 2. - Influence of cavitation on thrust and torque coefficients of the propeller P1380. P/D=1.188. J=0.6 (left), J=0.2 (right).

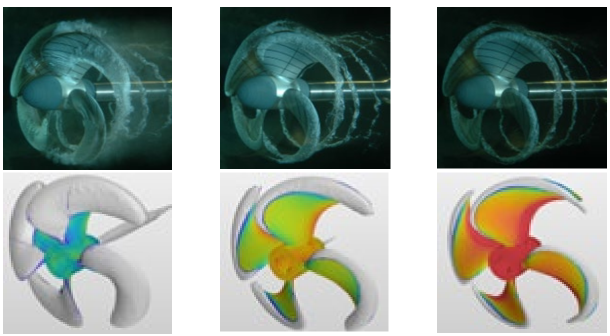

$\sigma_{\eta D}$ = 1.5 $\sigma_{\eta D}$ = 3.0 $\sigma_{\eta D}$ = 4.0

Figure 1. - Observed and computed cavitation extents on the propeller P1380 at different cavitation numbers. P/D=1.188. J=0.2

A pushing pod with a ducted *CP* propeller (P1374) was simulated with unsteady SM to capture rotor–stator interaction. The wall-resolved default mesh (≈18.2M cells, $y+$ ≈1) was advanced for ~20 revolutions at 2°/step in uniform inflow without cavitation. Pitch settings P/D={1.1,0.9,0.6,0.3,0.0} were tested (11 Hz, except 9 Hz at bollard, J=0). Agreement with experiments is good for $P/D \geq 0.6$ across total thrust, duct thrust, torque and efficiency (Figures 4-5). At low pitch, CFD under-predicts thrust/efficiency; the paper attributes this to gap-flow between hub and gondola (difficult to control in EFD and to model in CFD). Notably, at higher P/D the rotor–duct–pod interaction promotes transition, making fully-turbulent CFD closer to EFD than in the open-propeller case.

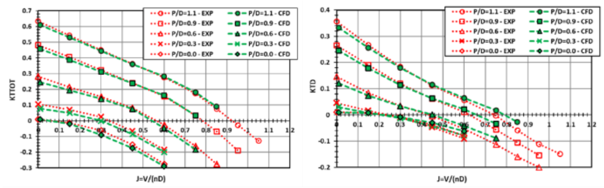

Figure 2. - Total thrust (left) and duct thrust (right) coefficients of the ducted azimuth thrust at different pitch settings of *CP* propeller.

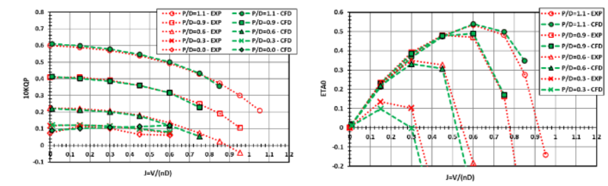

Figure 5. Propeller torque coefficient (left) and unit open water efficiency (right) of the ducted azimuth thrust at different pitch settings of CP propeller.

REFERENCES

Krasilnikov, V. I., & Di Paolo, B. (2025). Automated CFD tools for the design of marine propulsion systems. SINTEF Ocean & ENGYS.

ENGYS Limited. (2024). HELYX® 4.2.0 — HELYX-Core User's Guide. London, UK.

Berchiche, N., Krasilnikov, V. I., & Koushan, K. (2018). Numerical analysis of azimuth propulsor performance in seaways. Journal of Marine Science and Engineering, 6, 37.

Krasilnikov, V. I. (2024). Design exploration with counter-rotating propellers for a zero-emission coaster vessel. In Proc. 8th Int. Symp. on Marine Propulsors (SMP'24).

ACKNOWLEDGEMENT

This work was conducted as part of the Propeller Forum Phase III R&D project, funded by the Research Council of Norway.